Bull. Nov. Comp. Center, Num. Anal., 14 (2009), 95–114

Numerical simulation of plasma using the hybrid MHD-kinetic model*

L.V. Vshivkova

Abstract. In this paper, a numerical model for the propagation of the shear Alfven waves (SAWs) on open magnetic field lines using a hybrid kinetic approach is presented.

There is a two-dimensional hybrid model: an ion component of plasma is described by a standard set of the MHD equations, while electrons are taken into account via the Vlasov equation. To solve the Vlasov equation, a particle-in-cell method (PIC) is used, and for solving the MHD and the Maxwell equations, finite difference methods are utilized.

The problem is as follows. A region of an inhomogeneous magnetic field is defined in the Earth's polar area. At the initial time, the Alfven wave arrives in this region and causes a disturbance in electron distribution function velocities. The problem is to find an electron distribution function and fields as the wave propagates along the field.

1. Introduction

This paper deals with a problem of the modeling of the dynamics of solar wind particles in the Earth's magnetic field.

The interaction of solar wind particles with the Earth's magnetic field is of major interest in problems of the space physics. These energy-charged particles, when reaching the upper atmosphere of the Earth, give rise to one of the most spectacular phenomena in the night sky, the northern lights. Under the influence of the solar wind, the Earth magnetosphere becomes asymmetrical and stretches in the anti-solar direction. The northern lights on the night side of the Earth are associated with processes in the inner part of the magnetosphere. On the day side, plasma of the solar wind reaches the upper atmosphere through the open magnetic field lines.

The problem of modeling of processes in the magnetosphere can be solved by computing the interaction of the solar wind and the Earth's magnetic field. The non-stationary modeling is the most important one as the northern lights and magnetic storms, observed on the Earth, are due to changes in the distribution of plasma and the magnetic field in the magnetosphere.

In [31], the dispersive shear Alfven waves on the dipolar magnetic field lines are considered. In this work, a nonlinear model of the excitation of

*Supported by RFBR under Grants 08-01-615 and 08-01-622.

density perturbations and parallel electric fields by these waves are presented. It was found that a dispersion and nonlinearity define a depth, a spatial structure, and a growth of density fluctuations of a large amplitude at polar ionospheres. In the example given in this paper, a parallel potential drop was too small to interpret the acceleration of charged particles to high energies that can excite aurora. The ratio of the ion and the electron temperatures was $T_i/T_e = 3.3$. However, the authors mention if the ratio of the ion temperature to the electron temperature can be taken lower, then it will greatly increase a parallel electric field and a parallel potential drop.

In [36], the authors consider a nonstationary kinetic electron response to an electric current, which is driven by a standing shear Alfven wave. Here, also, plasma with an inhomogeneous (dipolar) magnetic field is considered. It was found that one of the mechanisms controlling the electron response to the field aligned currents of a low frequency is a mirror force leading to a parallel electric field (within regions of a large parallel magnetic field and a low plasma density), and another one is the quasistatic electric field along the magnetic field. Also, it is shown that there is no dependance on the magnitude of the parallel current in the energy of accelerated charged particles. The authors estimate that the amplitude of the field aligned current of 1 $\mu A/m^2$ results in parallel electric fields of 1 mV/m.

A model describing the nonlinear interaction between the dispersive shear Alfven wave field line resonances and the ion acoustic waves is presented in [13]. The limits of low-β ($\beta < m_e/m_i$) and high-β plasma were considered. In the former case, the electron inertia is dominant, and in the latter the electron thermal pressure effect is important. The analysis presented in this paper was based on a box model in which plasma parameters do not vary along the magnetic field lines. However, in fact, the geomagnetic field lines are curved and the parameters of plasma change from the ionosphere to the equatorial plane. Nevertheless, the authors note that the basic features of the model should be appropriate in a real geometry.

The papers mentioned above confirm that the development of numerical simulations of nonlinear effects in geometry, which is close to the real geometry of geomagnetic field lines is of major interest in the problems of space physics.

The method of discrete simulation is the most universal approach in the problems of collisionless plasma. Its first one-dimensional model was presented in [11]. The subsequent development of such models resulted in the particle-in-cell (PIC) method [3, 16, 17, 20]. In the PIC simulations, plasma is represented as a number of model particles, whose trajectories are characteristics of the Vlasov equation. Particles move according to the laws of classical mechanics in the self-consistent electromagnetic field to be found from the Maxwell equations.

In this paper, a numerical hybrid MHD-kinetic model for the shear Alfven waves propagation (SAWs) on the open magnetic field lines is presented. An ion component of plasma is described by a standard set of the MHD equations and electrons are via the Vlasov equation.

2. A parallel electric field in Space

One of the most important problems in the space physics is the acceleration of electrons in the auroral region. Kinetic energies of precipitating electrons reach high values of tens keV. In a period of many years, many different possible accelerator mechanisms were proposed. Among particle accelerators, there were proposed such mechanisms as double layers [1], magnetic mirrors [22], anomalous resistivity [34], kinetic Alfven waves [14,15,18,23,24,32,35], electrostatic shocks [27] and electrostatic turbulence [6,7].

The existence of a parallel electric field $E_{\|}$ was first predicted by Hannes Alfven, but for a long time it was commonly believed that a field-aligned component of the magnetospheric electric field can be neglected. The debate was that charged particles easily propagate along the magnetic field lines, and that any electric field would be nullified by contributions of ions and electrons, which are transported in different directions by this electric field. However, observations from a sounding rocket [26] have confirmed that $E_{\|}$ does occur in the Earth's magnetosphere, and that bright auroras are caused by the magnetospheric electrons, which are accelerated by this electric field. Also, these electrons carry a parallel (field-aligned) current $j_{\|}$ flowing upward. Observations of the parallel electric field in the upward current region are considered in [28].

In the case of an inhomogeneous magnetic field, it has to be shown that plasma supporting parallel electric field can maintain quasineutrality [33].

In [10], the expression for the parallel electric field is derived from the Ampere and the Farady laws giving

$$\frac{\partial^2 E_z(\boldsymbol{x})}{\partial x^2} - \frac{E_z(\boldsymbol{x})}{\lambda_e^2} = \frac{\partial(\nabla \cdot \boldsymbol{E}_\perp)}{\partial z} + \mu_0 e \frac{\partial}{\partial z} \sum v_i^2 S(\boldsymbol{x}, \boldsymbol{x}_i). \tag{1}$$

The same expression for the electric field is derived in [21]. If the last summand on the right-hand side of this equation is neglected, then equation (1) and the equations of the two-dimensional cold plasma approximation are self-consistent. However, for the electric field generation, the second term on the right has to be taken into account [10]. In this case, one more relation for the electric field has to be satisfied

$$\epsilon_0 \frac{\partial}{\partial t}(\nabla \cdot \boldsymbol{E}) = -\nabla \cdot \boldsymbol{j}. \tag{2}$$

That is, if the condition of quasineutrality, $n_e \approx n_i$, is initially assumed (at $t = 0$), then it will be preserved only if equation (2) is enforced. Otherwise, errors in $n_i - n_e$ will go unstable, causing the growth of the electric field $\boldsymbol{E}$. Equation (2) is the result of combining the electron and the ion continuity equations $\frac{\partial(n_i - n_e)}{\partial t} + \nabla \cdot (n_i \boldsymbol{v}_i - n_e \boldsymbol{v}_e) = 0$, the Poisson equation $\nabla \cdot \boldsymbol{E} = \frac{e}{\epsilon_0}(n_i - n_e)$ (where $\boldsymbol{E} = -\nabla\Phi$, Φ is a potential), and the expression for the current $\boldsymbol{j} = e(n_i \boldsymbol{v}_i - n_e \boldsymbol{v}_e)$.

3. Hybrid simulation techniques

For any simulation technique, where one of a plasma species is kinetically treated and another one as a fluid, the term of "hybrid code" is used. Here the first species is described by the Vlasov equation, while for the other one the MHD equations are used. Plasma can be coupled with electric and magnetic fields through the Maxwell equations. The most common model of a hybrid code in space plasmas is to kinetically treat ions and electrons as a fluid (see, e.g., [39]). These models have many successful applications in problems of collisionless plasma. However, in problems, where the wave-particle interactions become of the major interest, another approach for a hybrid code should be used. Namely, this means to treat electrons as particles and ions as a fluid.

3.1. A standard MHD-kinetic approach. Hybrid MHD-kinetic approaches, in which ions are kinetically treated and electrons are considered to be a fluid have been widely used in problems of the space physics. This type of models arose to simulate phenomena which occur at shorter scales than it can be interpreted by magnetohydrodynamics. Magnetohydrod dynamics cannot resolve processes at electron scales, such as the electron gyro-radius and the electron Debye length scales.

The ions in this model are described by the kinetic Vlasov equation

$$\frac{\partial f_\alpha}{\partial t} + \boldsymbol{v}\frac{\partial f_\alpha}{\partial \boldsymbol{r}} + \frac{\boldsymbol{F}_\alpha}{m_\alpha}\frac{\partial f_\alpha}{\partial \boldsymbol{v}} = 0, \tag{3}$$

where $f_\alpha = f_\alpha(\boldsymbol{r}, \boldsymbol{v}, t)$ is the ion distribution function, and m_α is the ion mass. The subscript α in this equation denotes the kind of ions in the case of multi-component plasma. The force $\boldsymbol{F}_\alpha$ is determined by

$$\boldsymbol{F}_\alpha = Z_\alpha e(\boldsymbol{E} + \boldsymbol{v} \times \boldsymbol{B}) + \boldsymbol{R}_\alpha. \tag{4}$$

Here Z_α is the amount of ionization of ions of the kind α, e is the electron charge, $\boldsymbol{E}$ and $\boldsymbol{B}$ are electric and magnetic fields, respectively, and $\boldsymbol{R}_\alpha = -\frac{Z_\alpha e}{\sigma}\boldsymbol{j}$ represents the frictional force between ions of the kind α and electrons. From equation (3) and (4) we obtain the ion motion equations

$$m_\alpha \frac{d\boldsymbol{v}}{dt} = Z_\alpha e\,(\boldsymbol{E} + \boldsymbol{v} \times \boldsymbol{B}) + \boldsymbol{R}_\alpha, \qquad \frac{d\boldsymbol{r}}{dt} = \boldsymbol{v}. \tag{5}$$

These equations are similar to those in the tutorial [39]. The difference is that equations (5) are written down for the case of multi-component plasma as it is very important to take into account the correct model statement (see [5,37]). For the plasma with one type of ions, i.e., when $\alpha = 1$, equations (5) become the same as in [39].

The density and average velocity of ions of the kind α are determined from the ion distribution function f_α

$$n_\alpha = \int f_\alpha \, d\boldsymbol{v}, \qquad \boldsymbol{V}_\alpha = \frac{1}{n_\alpha} \int f_\alpha \boldsymbol{v} \, d\boldsymbol{v}.$$

The system of equations describing electrons is as follows (see [37])

$$\frac{\partial n_e}{\partial t} + \nabla \cdot (n_e \boldsymbol{V}_e) = 0,$$

$$m_e\Big(\frac{\partial \boldsymbol{V}_e}{\partial t} + (\boldsymbol{V}_e \cdot \nabla)\boldsymbol{V}_e\Big) = -e(\boldsymbol{E} + \boldsymbol{V}_e \times \boldsymbol{B}) - \frac{\nabla p_e}{n_e} + \boldsymbol{R}_e,$$

$$n_e\Big(\frac{\partial T_e}{\partial t} + (\boldsymbol{V}_e \cdot \nabla)T_e\Big) + (\gamma - 1)p_e \nabla \cdot \boldsymbol{V}_e = (\gamma - 1)(Q_e - \nabla \cdot \boldsymbol{q}_e),$$

where n_e and $\boldsymbol{V}_e$ are the density and velocity of electrons, m_e is the electron mass, $p_e = n_e T_e$ is the electron pressure, $\boldsymbol{R}_e$ is the frictional force between electrons and ions, T_e is the electron temperature, Q_e is the electron heating (as a result of collisions with ions), $\boldsymbol{q}_e = -k_1 \nabla T_e$ is a heat flow, k_1 is the heat conductivity coefficient and γ is the ratio of specific heats. Finally, the electromagnetic fields are described by Maxwell's equations

$$\nabla \times \boldsymbol{B} = \mu_0 \boldsymbol{j}, \qquad \nabla \times \boldsymbol{E} = -\frac{\partial B}{\partial t}, \qquad \nabla \cdot \boldsymbol{B} = 0.$$

Here $\boldsymbol{j}$ is the current density which in the case of multi-component plasma has the form

$$\boldsymbol{j} = e\Big(\sum_\alpha Z_\alpha n_\alpha \boldsymbol{V}_\alpha - n_e \boldsymbol{V}_e\Big).$$

In the case of quasi-neutral plasma

$$n_e = \sum_\alpha Z_\alpha n_\alpha,$$

the Poisson equation $\nabla \cdot \boldsymbol{E} = e(n_i - n_e)/\epsilon_0$ is not included into the system.

3.2. Kinetic–electron and fluid–ion models. It was shown that the description of MHD is not valid when the problem of wave-particle interaction is considered [30]. In these problems, hybrid techniques should be used [38]. However, standard hybrid MHD-kinetic models, i.e., models where ions are kinetically described and electrons are considered to be a fluid, are not appropriate either, as this approach also removes the kinetic wave-particle electron effects. Consequently, a hybrid model that represents electrons as particles and ions as a fluid should be used.

There are different particle-electron and fluid-ion approaches with different assumptions. For example, the authors [25] have numerically realized a model which was first proposed in [29]. They considered an electrostatic model where an ion component of plasma was described by the equations of reduced magnetohydrodynamics. However, for the shear Alfven waves, the electromagnetic case is needed. In [21], a two-dimensional hybrid kinetic model of electron acceleration by the Alfven waves was presented. In this model a parallel ion motion was neglected. Also, in the equation of motion for electrons there is no μ term representing a mirror force.

Another hybrid MHD-kinetic model was considered in [10]. In this paper, a box model for the standing shear Alfven waves was considered. This model requires the use of the Poisson equation $\nabla \cdot \boldsymbol{E} = e(n_i - n_e)/\epsilon_0$ to find the correction electric field in order that a hybrid code be self-consistent. However, in the case of quasineutral plasma $n_i = n_e$ it is better to avoid the use of the Poisson equation.

In this paper, a two-dimensional electromagnetic model in a curvilinear geometry with allowance of a mirror force is considered.

4. Statement of the problem

Consider a two-dimensional problem of a shear Alfven wave propagation in the polar area of the Earth's magnetosphere. At the initial time $t = 0$, the Alfven wave (with the amplitude A and the frequency ω) comes into the region filled with plasma of constant density $n = n_0$ and a magnetic field of the dipolar type. While in motion, the wave disturbs the initial Maxwellian distribution function of electrons, forming a number of fast particles, which move towards the Earth.

4.1. The initial system of equations. We begin from the kinetic Vlasov equation (see, e.g., [2, 8, 19])

$$\frac{\partial f}{\partial t} + \boldsymbol{v} \cdot \frac{\partial f}{\partial \boldsymbol{r}} + \frac{q}{m}(\boldsymbol{E} + \boldsymbol{v} \times \boldsymbol{B})\frac{\partial f}{\partial \boldsymbol{v}} = 0, \tag{6}$$

where $f = f(t, \boldsymbol{r}, \boldsymbol{v})$ is a distribution function, q is a charge, m and $\boldsymbol{v}$ are the mass and velocity of a charged particle, $\boldsymbol{B}$ and $\boldsymbol{E}$ are a magnetic and an electric fields, respectively.

To describe the electron ($q = -e$) component of plasma in this problem, the gyro-averaged Vlasov equation (see, e.g., [19]) is used

$$\frac{\partial f}{\partial t} + \boldsymbol{v} \cdot \frac{\partial f}{\partial \boldsymbol{r}} - \frac{e}{m}\boldsymbol{E}\frac{\partial f}{\partial \boldsymbol{v}} = 0. \tag{7}$$

For electrons moving parallel to the background magnetic field $\boldsymbol{B}_0$, equation (7) becomes

$$\frac{\partial f}{\partial t} + v_r \frac{\partial f}{\partial r} - e v_r E_r \frac{\partial f}{\partial W} = 0, \tag{8}$$

where $f = f(t, r, W)$ is an electron distribution function, v_r is a particle velocity in the direction of the axis r, e is an electron charge, E_r is an r-component of the electric field $\boldsymbol{E}$, $W = \frac{1}{2}m_e v_r^2 + \mu B_r$ is a particle kinetic energy, m_e is an electron mass, $\mu = \frac{m_e v_\perp^2}{2B_r}$ is a magnetic moment and B_r is an r-component of the magnetic field $\boldsymbol{B}$. The magnetic moment μ is defined for each particle in a random way by assigning the transverse velocity according to the initial temperature. Later, this magnetic moment remains constant for a particle.

The motion of the ion component of plasma is described by a system of equations consisting of the continuity equation and the equation of motion in which a pressure gradient term was omitted (assumption of the cold plasma)

$$\frac{dn_i}{dt} + \nabla \cdot (n_i \boldsymbol{V}_i) = 0, \tag{9}$$

$$m_i \frac{d\boldsymbol{V}_i}{dt} = e[\boldsymbol{E} + \boldsymbol{V}_i \times \boldsymbol{B}], \tag{10}$$

where n_i and $\boldsymbol{V}_i$ correspond to the density and the average velocity of the ion component, m_i is the ion mass, $\boldsymbol{E}$ and $\boldsymbol{B}$ represent the electric and the magnetic fields, respectively.

To describe the electric and the magnetic fields, the Maxwell equations are used

$$\nabla \times \boldsymbol{E} = -\frac{\partial \boldsymbol{B}}{\partial t}, \tag{11}$$

$$\nabla \times \boldsymbol{B} = \mu_0 \boldsymbol{j}, \tag{12}$$

$$\nabla \cdot \boldsymbol{B} = 0. \tag{13}$$

Here $\boldsymbol{j} = ne(\boldsymbol{V}_i - \boldsymbol{V}_e)$ is a current density and μ_0 is a free space permeability. All the equations are written down in SI units.

There were made some assumptions in the problem. It is considered to be a quasi-neutral ($n_i = n_e = n$) plasma consisting of hydrogen ions and electrons. Also, it is assumed that there is a very strong magnetic field along the Alfven wave propagation which enables us to consider electrons moving

only in the direction parallel to the magnetic field. On the right-hand side of the Ampere law (12), the displacement current $\mu_0\epsilon_0\frac{\partial \boldsymbol{E}}{\partial t}$ was neglected as there are only low-frequency oscillations that are considered in this problem.

Finally, to avoid difficulties of the numerical calculation of the perpendicular component of the electric field E_ϕ from equation of motion (10), the assumption of $\boldsymbol{E}_\phi = -\boldsymbol{v}_i \times \boldsymbol{B}$ is made. That is, there are no whistler modes and only the shear Alfven wave modes are considered (see, e.g., [9]). In the next section, equations (16)–(18) show how this assumption is implemented along with equation (10).

5. Description of the algorithm

5.1. Initial data and boundary conditions. A two-dimensional flow in the plane (r, ϕ) with $\partial/\partial z = 0$ is considered. Figure 1 shows the geometry of the given problem. Here the coordinates r and ϕ correspond to the parallel and perpendicular directions to the background magnetic field B_0. Let us write down the system of equations in cylindrical coordinates with the assumptions made above.

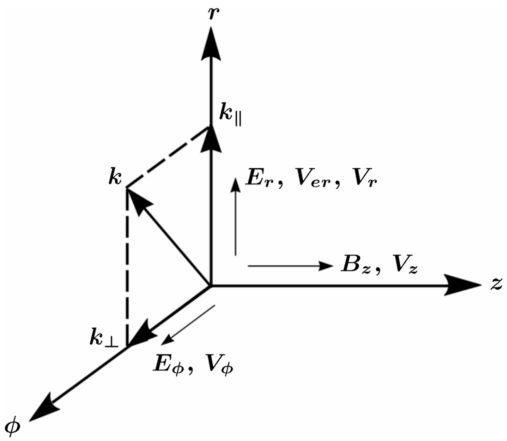

Figure 1. Geometry of the problem. The background magnetic field B_0 is along r direction

First, write all vectors component-wise. The average electron velocity $\boldsymbol{V}_e$ has only one coordinate in r-direction $\{V_{er}, 0, 0\}$, as electrons are moving only parallel to the background field. That is, we neglect $\boldsymbol{E} \times \boldsymbol{B}$-drift for electrons across the magnetic field. This assumption can be made as a strong magnetic field is considered in the problem, and the magnitude of this drift is proportional to E/B, which is very small when $E \ll B$. Ions can move in any direction, i.e., $\boldsymbol{V} = \{V_r, V_\phi, V_z\}$. The magnetic and the electric fields are $\boldsymbol{B} = \{B_0, 0, B_z\}$ and $\boldsymbol{E} = \{E_r, E_\phi, 0\}$, respectively. Equations (8)–(13) become

$$\frac{\partial f}{\partial t} + v_r\frac{\partial f}{\partial r} - ev_rE_r\frac{\partial f}{\partial W} = 0, \tag{14}$$

$$\frac{\partial n}{\partial t} + \frac{1}{r}\frac{\partial}{\partial r}(rnV_r) + \frac{1}{r}\frac{\partial}{\partial \phi}(nV_\phi) = 0, \tag{15}$$

$$m_i\left(\frac{\partial V_r}{\partial t} + V_r\frac{\partial V_r}{\partial r} + \frac{V_\phi}{r}\frac{\partial V_r}{\partial \phi} - \frac{V_\phi^2}{r}\right) = eE_r + eV_\phi B_z, \tag{16}$$

$$E_\phi = -V_z B_r + V_r B_z, \tag{17}$$

$$m_i\left(\frac{\partial V_z}{\partial t} + V_r\frac{\partial V_z}{\partial r} + \frac{V_\phi}{r}\frac{\partial V_z}{\partial \phi}\right) = eV_\phi B_r, \tag{18}$$

$$\frac{\partial B_z}{\partial t} = -\frac{1}{r}\frac{\partial}{\partial r}(rE_\phi) + \frac{1}{r}\frac{\partial E_r}{\partial \phi}, \tag{19}$$

$$\mu_0 j_r = \frac{1}{r}\frac{\partial B_z}{\partial \phi}, \qquad \mu_0 j_\phi = -\frac{\partial B_z}{\partial r}. \tag{20}$$

As illustrated in Figure 2, the solution is considered in the area

$$r_{\min} \le r \le r_{\max}, \qquad -\phi_{\max} \le \phi \le \phi_{\max}.$$

Here r and ϕ are the radial and the azimuthal directions, respectively; L_1 and L_2 are the length and the top width of the box.

As initial data, a non-perturbed state of plasma is used in the pole area of a magnetic dipole, that is

$$n = n_0, \quad B_\phi = 0, \quad B_z = 0, \quad B_r = B_r(r) \sim \frac{1}{r^3},$$
$$E_r = E_\phi = E_z = 0, \quad V_r = V_\phi = V_z = 0.$$

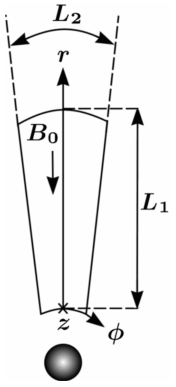

Figure 2

Now let us consider the boundary conditions of the problem formulated. On the left $\phi = -\phi_{\max}$ and on the right $\phi = \phi_{\max}$ boundaries of the box (Figure 2), the periodic boundary conditions are set. At the bottom boundary $r = r_{\min}$, all functions are equal to the values at the initial time. At the upper boundary $r = r_{\max}$ conditions of the incoming Alfven wave are set, using a simpler two-fluid set of equations. This will allow us to set a perpendicular $\boldsymbol{E}$-field and components of the above magnetic field.

The linearized system of equations in this case becomes as follows:

$$\frac{\partial n}{\partial t} = -n_0\Big(\frac{\partial V_r}{\partial r} + \frac{\partial V_\phi}{\partial \phi}\Big), \tag{21}$$

$$m_e\frac{\partial V_{er}}{\partial t} = -eE_r, \qquad m_i\frac{\partial V_r}{\partial t} = eE_r, \tag{22}$$

$$m_i\frac{\partial V_z}{\partial t} = -eB_0V_\phi, \qquad E_\phi = -B_0V_z, \tag{23}$$

$$\frac{\partial B_z}{\partial t} = -\frac{\partial E_\phi}{\partial r} + \frac{\partial E_r}{\partial \phi}, \tag{24}$$

$$\frac{\partial B_z}{\partial \phi} = \mu_0 n_0 e(V_r - V_{er}), \tag{25}$$

$$\frac{\partial B_z}{\partial r} = -\mu_0 n_0 e V_\phi. \tag{26}$$

This linearized system satisfies the following dispersion relation:

$$\omega^2 = \frac{k_\parallel^2 V_A^2}{1 + \lambda_e^2 k_\perp^2},$$

where ω is the wave frequency, $k_\parallel$ and $k_\perp$ are parallel and perpendicular wave numbers, respectively, V_A is the Alfven speed, $\lambda_e = c/\omega_{pe}$ is the electron inertial length or the electron skin depth, c is the speed of light and ω_{pe} is the electron plasma frequency. It can be easily derived if we substitute the dependence $f = \tilde{f}\exp(-i\omega t + ik_\parallel r + ik_\perp \phi)$ into equations (22)–(26). Here $f = \{V_r, V_\phi, V_z, V_{er}, B_z, E_r, E_\phi\}$.

Then, assuming that the perpendicular component of electric field $E_\phi = A\sin\psi$, where A is the amplitude of the wave at the boundary $r = r_{\max}$ and $\psi = -\omega t + k_\perp \phi + k_\parallel r$, from equations (21)–(26), we obtain the following expressions for the upper boundary:

$$E_\phi = A\sin\psi, \quad E_r = A\frac{k_\parallel}{k_\perp}\left(1 - \mu_0 n_0 e\frac{\omega^2}{k_\parallel^2}\right)\sin\psi, \quad B_z = A\mu_0 n_0 e\frac{\omega}{k_\parallel}\sin\psi,$$

$$V_\phi = -A\frac{m_i}{eB_0^2}\omega\cos\psi, \quad V_z = -\frac{A}{B_0}\sin\psi,$$

$$V_r = A\frac{e}{m_i}\frac{k_\parallel}{\omega k_\perp}\left(1 - \mu_0 n_0 e\frac{\omega^2}{k_\parallel^2}\right)\cos\psi,$$

$$V_{er} = -A\frac{e}{m_e}\frac{k_\parallel}{\omega k_\perp}\left(1 - \mu_0 n_0 e\frac{\omega^2}{k_\parallel^2}\right)\cos\psi,$$

$$n = -An_0\left[\frac{m_i}{eB_0^2}k_\perp - \frac{e}{m_i}\frac{k_\parallel^2}{\omega^2 k_\perp}\left(1 - \mu_0 n_0 e\frac{\omega^2}{k_\parallel^2}\right)\right]\cos\psi.$$

5.2. Normalization of the system. The normalized magnitudes in the problem are as follows: the background density n_0, non-perturbed magnetic field B_0, the electric field E_0, the Alfven velocity $V_A = \frac{B_0}{\sqrt{\mu_0 m_i n_0}}$, the ion plasma frequency $\omega_{pi} = \sqrt{\frac{n_0 e^2}{\varepsilon_0 m_i}}$, the length $L = \frac{c}{\omega_{pi}} = \frac{c\sqrt{\varepsilon_0 m_i}}{e\sqrt{n_0}}$, the time $t_0 = \frac{L}{V_A} = \frac{cm_i}{eB_0} = \frac{1}{\omega_{ci}}$, where ω_{ci} is the ion cyclotron frequency. The characteristic equations of the Vlasov equation (8) in dimensionless variables can be written down as

$$\frac{dr}{dt} = v_r, \qquad \frac{dW}{dt} = -\frac{1}{\beta}v_r E_r, \tag{27}$$

where $W = \frac{1}{2}(v_r^2 + v_\perp^2)$ and $\beta = \frac{m_e}{m_i}$, and the other equations from system (14)–(20) in dimensionless variables become as follows:

$$\frac{\partial n}{\partial t} + \frac{1}{r}\frac{\partial}{\partial r}(rnV_r) + \frac{1}{r}\frac{\partial}{\partial \phi}(nV_\phi) = 0, \tag{28}$$

$$E_\phi = -V_z B_r + V_r B_z, \tag{29}$$

$$\frac{\partial V_z}{\partial t} + V_r\frac{\partial V_z}{\partial r} + \frac{V_\phi}{r}\frac{\partial V_z}{\partial \phi} = V_r B_\phi - V_\phi B_r, \tag{30}$$

$$\frac{\partial V_r}{\partial t} + V_r\frac{\partial V_r}{\partial r} + \frac{V_\phi}{r}\frac{\partial V_r}{\partial \phi} - \frac{V_\phi^2}{r} = E_r + V_\phi B_z - V_z B_\phi. \tag{31}$$

$$\frac{\partial B_z}{\partial t} = \frac{1}{r}\frac{\partial E_r}{\partial \phi} - \frac{1}{r}\frac{\partial}{\partial r}(rE_\phi), \tag{32}$$

$$V_\phi = -\frac{1}{n}\frac{\partial B_z}{\partial r}, \qquad V_{er} = V_r - \frac{1}{nr}\frac{\partial B_z}{\partial \phi}. \tag{33}$$

A uniform scheme with the steps h_1 and h_2 on the axes ϕ and r, respectively, is introduced into the calculated area (Figure 3). Black dots denote mesh nodes. Solid and dashed line dots are centers of cells and of mesh boundaries, respectively.

The magnetic field B_z is defined at the grid nodes $(\phi_i,\ r_k)$, the functions V_ϕ, E_ϕ, B_r, j_ϕ — at the points $(\phi_i,\ r_{k-1/2})$, the functions V_r, E_r, j_r — at the points $(\phi_{i-1/2},\ r_k)$, and the functions n_i, V_z, E_z — in the centers of the cells $(\phi_{i-1/2},\ r_{k-1/2})$. Here $\phi_\alpha = \alpha h_1$, $r_\beta = \beta h_2$.

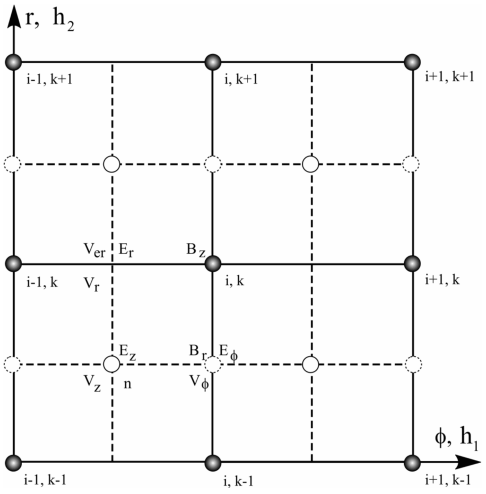

Figure 3. The grid

5.3. The calculation technique of a parallel electric field. The main difficulty in this algorithm is to calculate the electric field E_r, which is parallel to the background magnetic field B_0. This electric field is determined from the electron motion equation (8) by the particle-in-cell (PIC) method (see, e.g., [20]).

As the field E_r acting on a particle is interpolated into the particle location, the velocity V_{er} at the mesh nodes depends on values of E_r in the surrounding nodes. Therefore, there is a system of linear algebraic equations for determination of E_r. Fifteen values are connected with each other

in each equation of this system. For every node, we obtain the equation of the form

$$V_{er} = f(E_r). \tag{34}$$

The method for obtaining this system of equations will be described below. First, let us consider the derivation of the formula for calculation of the parallel electric field.

For each particle, the characteristic equations of the Vlasov equation (27) can be written down as

$$\frac{dv_{r,j}}{dt} = -\frac{1}{\beta}E_r(\phi_j, r_j) - \mu_j \frac{\partial B_r(\phi_j, r_j)}{\partial r}, \qquad \frac{dr_j}{dt} = v_{r,j}.$$

Here the magnetic moment of each particle μ_j is defined before calculation and remains constant. The difference scheme for these equations is as follows:

$$v_{r,j}^{m+1} = v_{r,j}^{m} - \frac{\tau}{\beta}E_{r,j}^{m+1} - \mu_j \tau \Big(\frac{\partial B_r}{\partial r}\Big)_j^m, \tag{35}$$

$$r_j^{m+1} = r_j^m + \tau v_{r,j}^{m+1}, \tag{36}$$

where $\beta = \frac{m_e}{m_i}$, j is the particle number,

$$E_{r,j} = \sum_{i,k} E_{r,i-1/2,k} R(\phi_{i-1/2} - \phi_j) R(r_k - r_j) \tag{37}$$

and $R(f)$ is the following function (see, e.g., [4]):

$$R(f) = \max\Big(1 - \frac{|f|}{h},\ 0\Big),$$

where $f = \{\phi, r\}$ and $h = \{h_1, h_2\}$. Introducing the notation

$$D_{i,k} \equiv \Big(\frac{\partial B_r}{\partial r}\Big)_{i,k} = \frac{1}{h_2}\big(B_{r,i,k+1/2}^{m+1} - B_{r,i,k-1/2}^{m}\big),$$

we can write down

$$\Big(\frac{\partial B_r}{\partial r}\Big)_j = \sum_{i,k} D_{i,k} R(\phi_i - \phi_j) R(r_k - r_j). \tag{38}$$

The density and the current density of electrons are

$$n_{e,i-1/2,k} = \sum_j m_j R(\phi_{i-1/2} - \phi_j) R(r_k - r_j),$$

$$(n_e V_{er})_{i-1/2,k} = \sum_j v_{r,j} m_j R(\phi_{i-1/2} - \phi_j) R(r_k - r_j).$$

Consequently, using the latter two equations, we arrive at the formula for calculating the electron velocity at the time point t^{m+1}

$$V_{er,i-1/2,k}^{m+1} = \frac{1}{N_{i-1/2,k}^{m+1}} \sum_j v_{r,j}^{m+1} R\big(\phi_{i-1/2} - \phi_j^{m+1}\big) R\big(r_k - r_j^{m+1}\big), \qquad (39)$$

where

$$N_{i-1/2,k}^{m+1} = \sum_j R\big(\phi_{i-1/2} - \phi_j^{m+1}\big) R\big(r_k - r_j^{m+1}\big).$$

Then, substituting $v_{r,j}^{m+1}$ from equation (35), we have the following expression:

$$\begin{aligned}
\frac{\tau}{\beta} \sum_j E_{r,j} R\big(\phi_{i-1/2} - \phi_j^{m+1}\big) R\big(r_k - r_j^{m+1}\big) \\
= \sum_j v_{r,j}^{m} R\big(\phi_{i-1/2} - \phi_j^{m+1}\big) R\big(r_k - r_j^{m+1}\big) - \\
\tau \sum_j \mu_j \Big(\frac{\partial B_r}{\partial r}\Big)_j R\big(\phi_{i-1/2} - \phi_j^{m+1}\big) R\big(r_k - r_j^{m+1}\big) - \\
V_{er,i-1/2,k}^{m+1} N_{i-1/2,k}^{m+1}. \qquad (40)
\end{aligned}$$

Introduce the notation of the right-hand side of this equation as $F_{i-1/2,k}$. Then equation (40) becomes

$$\frac{\tau}{\beta} \sum_j E_{r,j} R\big(\phi_{i-1/2} - \phi_j^{m+1}\big) R\big(r_k - r_j^{m+1}\big) = F_{i-1/2,k}.$$

Afterwards, substituting $E_{r,j}$ from (37) into the left-hand side of this equation we come to

$$\begin{aligned}
\frac{\tau}{\beta} \sum_j R\big(\phi_{i-1/2} - \phi_j^{m+1}\big) R\big(r_k - r_j^{m+1}\big) \times \\
\sum_{i',k'} R\big(\phi_{i'-1/2} - \phi_j^{c}\big) R\big(r_{k'} - r_j^{c}\big) E_{r,i'-1/2,k'} = F_{i-1/2,k}.
\end{aligned}$$

Here, i' and k' are introduced in order to differ from i and k, which are used in the first part of this equation. Also, $r_j^c = (r_j^{m+1} + r_j^m)/2$. Rearranging this equation in the form

$$\begin{aligned}
\frac{\tau}{\beta} \sum_{i',k'} E_{r,i'-1/2,k'} \sum_j R\big(\phi_{i-1/2} - \phi_j^{m+1}\big) R\big(r_k - r_j^{m+1}\big) \times \\
R\big(\phi_{i'-1/2} - \phi_j^{c}\big) R\big(r_{k'} - r_j^{c}\big) = F_{i-1/2,k}, \qquad (41)
\end{aligned}$$

we obtain the final formula for calculation of the parallel electric field.

Now, let us consider the method used for obtaining the system of equations equations (34). Let V_{er} and E_r be defined at the grid nodes (i, k).

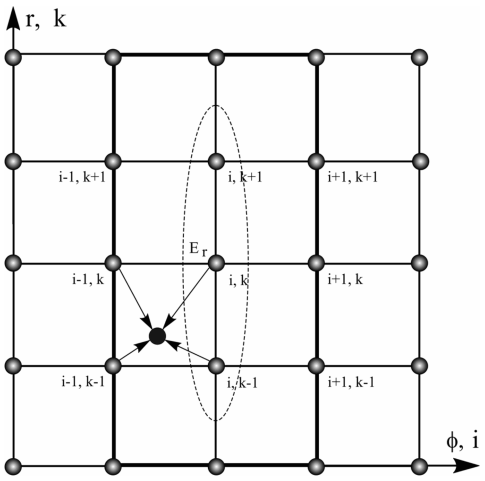

Figure 4. The 15-point pattern. The black dot inside a cell denotes a particle

At the time point t^{m+1}, the velocity of electrons V_{er} is defined by velocities of particles which are in the cells surrounded by the grid nodes $(i-1,k-1)$, $(i+1,k-1)$, $(i-1,k+1)$, and $(i+1,k+1)$ (Figure 4). The particles, which are in these four cells at the time point t^{m+1}, at the previous time point t^m could be in any eight cells surrounded by the grid nodes $(i-1,k-2)$, $(i+1,k-2)$, $(i-1,k+2)$, and $(i+1,k+2)$. It follows from the fact that particles can move only in the r-direction and cross the cell boundaries during the time step τ. There is, also, an electric field E_r, which is defined in the grid nodes of these eight cells, acting on the particles, located in these eight cells at the time point t^m.

We can write equation (35) for each particle defining V_{er} in the grid nodes. Then, after substitution it into equation (39), we arrive at the following equation:

$$\begin{aligned} N_{i,k}^{m+1}V_{er,i,k}^{m+1} = {} & R_{i,k}^{11}E_{r,i-1,k-2}^{m+1} + R_{i,k}^{12}E_{r,i,k-2}^{m+1} + R_{i,k}^{13}E_{r,i+1,k-2}^{m+1} + \\ & R_{i,k}^{21}E_{r,i-1,k-1}^{m+1} + R_{i,k}^{22}E_{r,i,k-1}^{m+1} + R_{i,k}^{23}E_{r,i+1,k-1}^{m+1} + \\ & R_{i,k}^{31}E_{r,i-1,k}^{m+1} + R_{i,k}^{32}E_{r,i,k}^{m+1} + R_{i,k}^{33}E_{r,i+1,k}^{m+1} + \\ & R_{i,k}^{41}E_{r,i-1,k+1}^{m+1} + R_{i,k}^{42}E_{r,i,k+1}^{m+1} + R_{i,k}^{43}E_{r,i+1,k+1}^{m+1} + \\ & R_{i,k}^{51}E_{r,i-1,k+2}^{m+1} + R_{i,k}^{52}E_{r,i,k+2}^{m+1} + R_{i,k}^{53}E_{r,i+1,k+2}^{m+1} + Q_{i,k}^{m}. \end{aligned} \quad (42)$$

Here the coefficients R^{11}, R^{12}, …, R^{53} are obtained by summation of coefficients of E_r from each particle. The term $Q_{i,k}$ results from summation of the last summands in equation (35) and particle velocities at the point time t^m. In equation (42), the terms $N_{i,k}^{m+1}V_{er,i,k}^{m+1}$ and $Q_{i,k}^{m}$ are known, and terms with electric field E_r are unknown.

Thus, we obtain the system of liner algebraic equations to determine E_r in the grid nodes. This system is solved by the following manner. The terms $E_{r,i,k-1}^{m+1}$, $E_{r,i,k}^{m+1}$, and $E_{r,i,k+1}^{m+1}$ with values in the three central nodes (the nodes cycled with a dashed line in Figure 4) of the fifteen-point pattern (the thick line pattern) are transferred to the left side of the system and the rest terms — to the right-hand side. After this procedure for each i we come to the system with a three-diagonal matrix which is solved using

the double-sweep method. This method is stable as we attain the diagonal dominance in the system.

5.4. A quasi-neutrality and numerical noise. In this method, the ion density n_i is defined from equation (28). Because of the assumption of quasi-neutral property, the ion and the electron densities must coincide: $n_i = n_e$. However, if we calculate the electron density by the formula

$$n_{i-1/2,k-1/2} = \sum_j m_j R(\phi_{i-1/2} - \phi_j) R(r_{k-1/2} - r_j),$$

where $R(x) = \max\Big(1 - \frac{|x|}{h},\ 0\Big)$, we will not obtain the required equality. This is because of discreteness of a time step and insufficient number of particles. Therefore, there is a necessity in the adjustment of particle location to enforce the quasi-neutral property. A one-dimensional case of this adjustment is presented in [12]. In similar manner, this adjustment is realized by iterations along ϕ and r for the current two-dimensional case.

Because of a limited number of model particles, there are phenomena that are not associated with the physics of simulated processes. The discreteness of model particles in calculations leads to such effects as an increase of the number of collisions, non-conservation of energy, etc. To remedy this, the algorithm of the numerical noise reduction, presented in [12], is used.

6. Test runs

In this section, the simulation results of the Alfven wave dynamics are presented. The Alfven wave is specified on the boundary $r = r_{\max}$. For the test runs presented below, the following parameters are chosen: the length of the simulation box is $L_1 = 200$ km, the width is $L_2 = 40$ km (see Figure 2). Also, in order to ensure that the background magnetic field $\boldsymbol{B}_0$, is uniform, the distance from the center of the Earth to the bottom boundary of the simulation box was taken to be 637,000 km, which is approximately equal to $100R_E$, where R_E is the Earth's radius. The magnitude of the background magnetic field is $B_0 = 66.6$ nT, the density $n_0 = 3 \cdot 10^5$ m^{-3} and the temperature of electrons $T_e = 10$ eV. The latter parameters have been chosen in such a way that $k_\perp \lambda_e = 2.5$ and $v_{the}^2/V_A^2 = 0.5$. The Alfven speed corresponding to these parameters is $v_A = 2652$ km/s and the thermal speed is 1876 km/s.

The simulation parameters are as follows: the number of particles is $N = 500{,}000$ and the number of cells in the perpendicular and in the parallel directions are 32 and 64, respectively. Consequently, there are 2048 cells and 244 particles per cell.

In Figures 5–7, the contour plots show the wave propagation in the considered area. A wave comes into the box from the above boundary and

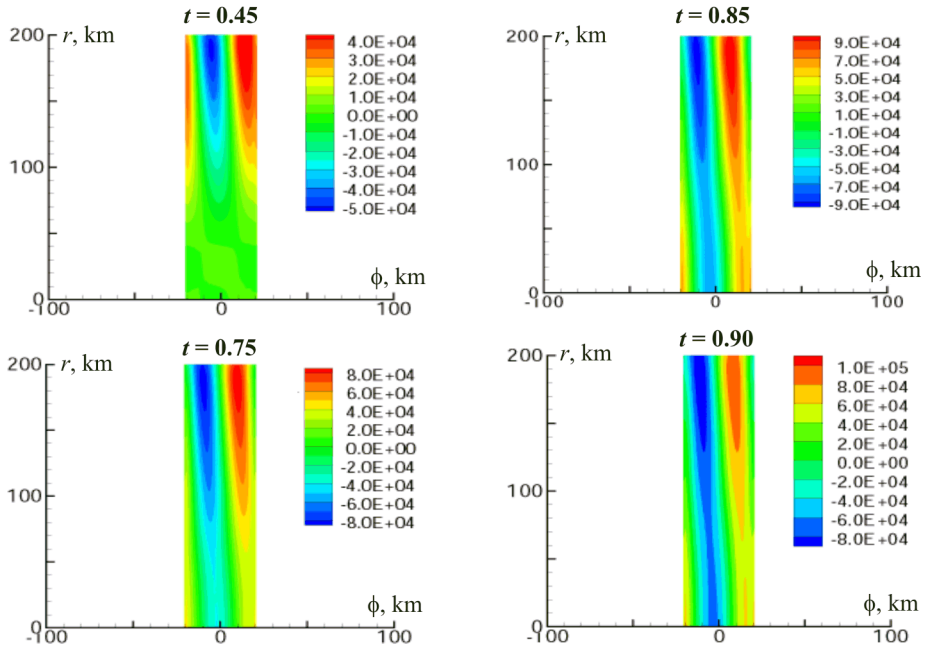

Figure 5. The electron velocity

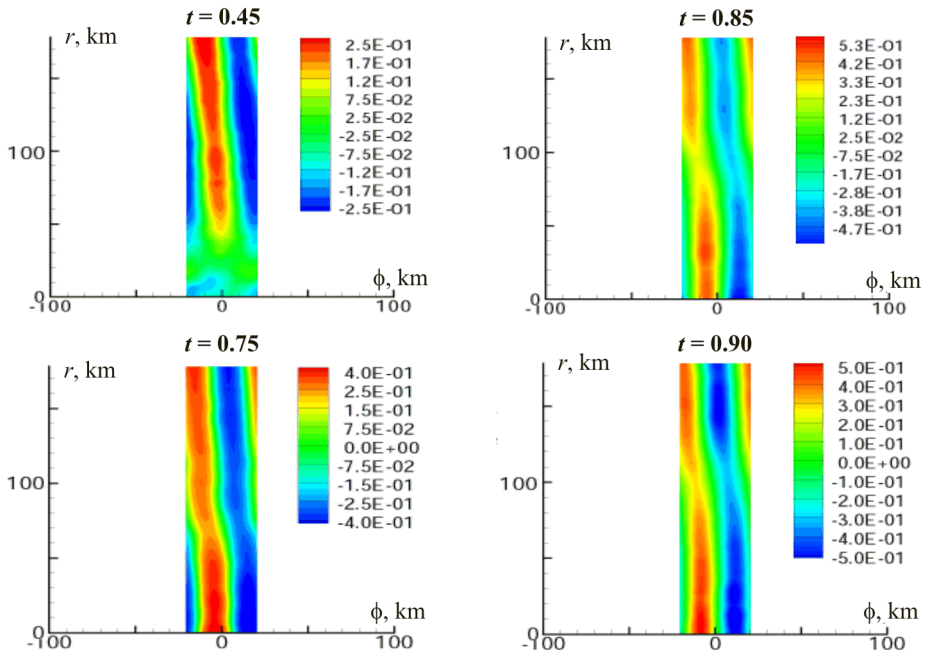

Figure 6. The propagation of the electric field along r-axis

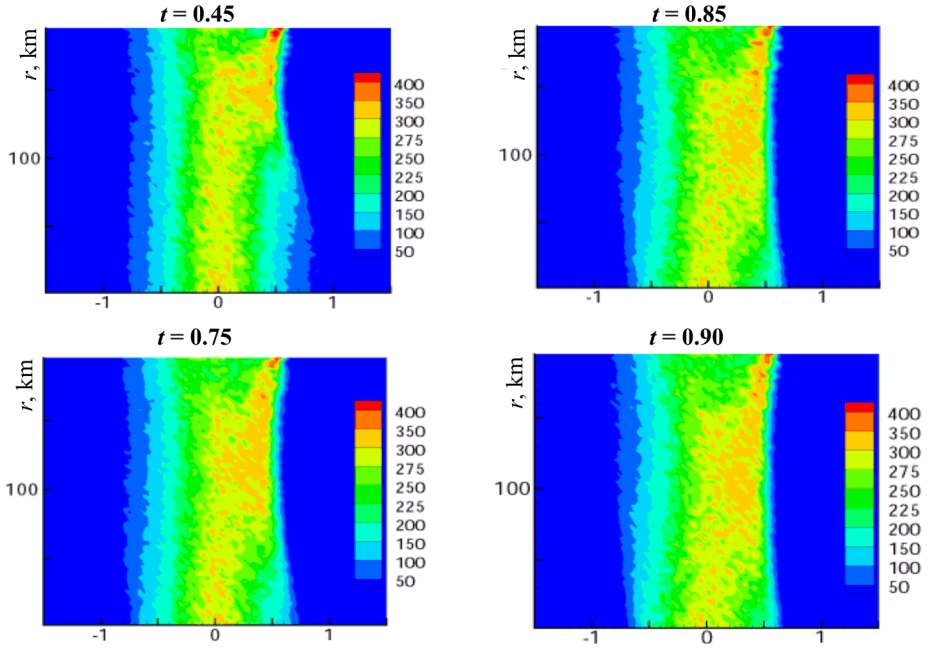

Figure 7. The evolution of the electron distribution function

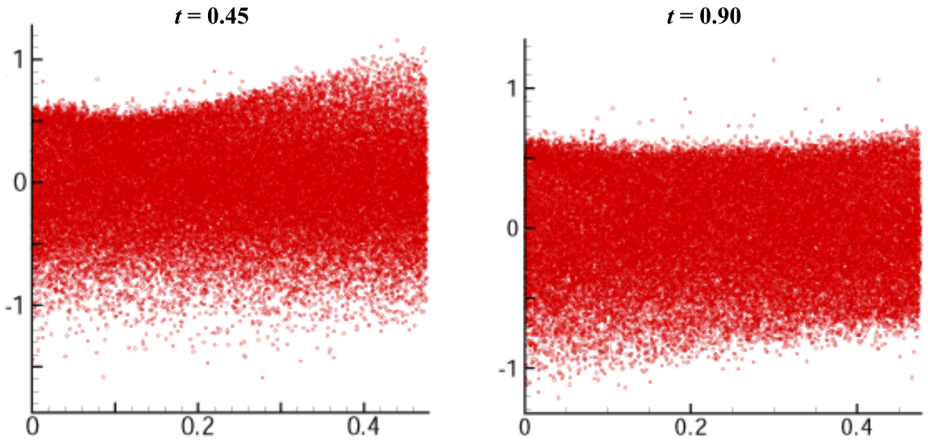

Figure 8. The phase space

propagates downward. The plots were taken at the dimensionless time steps $t = 0.45$, 0.75, 0.85, and 0.9. From these figures one can see that the wave is propagating downward smoothly and is reflecting at the bottom boundary. These plots illustrate the evolution of the electron velocity (see Figure 5), the parallel electric field (see Figure 6) and the electron distribution function (see Figure 7). From the plots of the phase space (Figure 8) one can see how the wave affects the particles in the considered region.

7. Conclusion

In this paper, the new two-dimensional hybrid model for the modeling of a charged particle motion in the polar area of the Earth's magnetic field is presented. In this model, the ion component of plasma is described by the MHD equations, while the electron component is taken into account for via the Vlasov equation. The electric and the magnetic fields are found from the Maxwell equations. In this paper, the algorithms for finding a parallel electric field by particle velocities are described in greater detail than in [12] and the boundary conditions at the upper boundary are corrected. Also, more appropriate parameters were found to obtain the results demonstrated in [12]. Here, the test runs for the uniform background magnetic field $\boldsymbol{B}_0$ are presented. However, with a more careful choice of parameters it is possible to simulate the processes in a curvilinear geometry.

Acknowledgements. I would like to thank R. Rankin, R. Marchand and C. Watt from the University of Alberta, and G.I. Dudnikova from the ICT SB RAS for useful discussions and their suggestions in choosing physical parameters for solving this problem.

References

[1] Alfven H. On the theory of magnetic storms and aurorae // Tellus. — 1958. — Vol. 10, No. 1. — P. 104–116.

[2] Baumjohann W., Treumann R.A. Basic Space Plasma Physics. — Imperial College Press, 1996.

[3] Berezin Yu.A., Vshivkov V.A. The Method of Particles in the Dynamics of Low-Density Plasma. — Novosibirsk: Nauka, 1980.

[4] Birdsall C.K., Langdon A.B. Plasma Physics via Computer Simulation. — Bristol: Hilger, 1991.

[5] Braginskii S.I. Transport processes in plasma // Vopr. Teor. Plasmy. — 1963. — Vol. 1. — P. 183–272 (English transl. Reviews of Plasma Physics. — 1965. — Vol. 1. — P. 205).

[6] Bryant D.A., Cook A.C., Wang Z.-S., de Angelis U., Perry C.H. Turbulent acceleration of auroral electrons // J. Geophysical Research. — 1991. — Vol. 96, No. A8. — P. 13829–13839.

[7] Bryant D.A. Electron acceleration in the aurora // Contemporary Physics. — 1994. — Vol. 35. — P. 165–179.

[8] Chen F.F. An Introduction to Plasma Physics and Controlled Fusion. — Plenum Press, 1984.

[9] Cross R.C. An Introduction to Alfven Waves. — Taylor & Francis, 1988.

[10] Damiano P.A., Sydora R.D., Samson J.C. Hybrid magnetohydrodynamic-kinetic model of standing shear Alfven waves // J. Plasma Physics. — 2003. — Vol. 69, Part 4. — P. 277–304.

[11] Dawson J. One-dimensional plasma model // Physics of Fluids. — 1962. — Vol. 5, No. 4. — P. 445–459.

[12] Dudnikova G.I., Vshivkova L.V., Rankin R. Hybrid model of a share Alfven wave propagation in collisionless plasma // Computational Technologies. — 2006. — Vol. 11, No. 3. — P. 50–60.

[13] Frycz P., Rankin R., Samson J.C., Tikhonchuk V.T. Nonlinear field line resonances: Dispersive effects // Physics of Plasmas. — 1998. — Vol. 5, No. 10. — P. 3565–3574.

[14] Goertz C.K. Discrete breakup arcs and kinetic Alfven waves / S.-I. Akasofu and J.R. Kan, eds. // Physics of Auroral Arc Formation. — Washington D.C.: AGU, 1981. — — P. 451–456, (Geophysical Monograph Series; 25).

[15] Goertz C.K., Boswell R.W. Magnetosphere-ionosphere coupling // J. Geophysical Research. — 1979. — Vol. 84, No. A12. — P. 7239–7246.

[16] Grigoryev Yu.N., Vshivkov V.A. Numerical particle-in-cell methods. — Novosibirsk: Nauka, 2000.

[17] Grigoryev Yu.N., Vshivkov V.A., Fedoruk M.P. Numerical "Particle-in-Cell" Methods. Theory and Applications. — Utrecht–Boston: VSP, 2002.

[18] Hasegawa A. Particle acceleration by MHD surface wave and formation of aurora // J. Geophysical Research. — 1996. — Vol. 81. — P. 5083–5090.

[19] Hazeltine R.D., Waelbroeck F.L. The Framework of Plasma Physics. — Perseus Books, 1998.

[20] Hockney R.W., Eastwood J.W. Computer Simulation Using Particles. — McGraw-Hill Education, 1981.

[21] Hui C.H., Seyler C.E. Electron acceleration by Alfven waves in the magnetosphere // J. Geophysical Research. — 1992. — Vol. 97. — P. 3953–3963.

[22] Knight S. Parallel electric fields // Planetary and Space Science. — 1973. — Vol. 21, Iss. 5. — P. 741–750.

[23] Lysak R.L., Carlson C.W. Effect of microscopic turbulence on magnetosphere-ionosphere coupling // Geophysical Research Letters. — 1981. — Vol. 8. — P. 269–272.

[24] Lysak R.L., Dum C.T. Dynamics of magnetosphere-ionosphere coupling including turbulent transport // J. Geophysical Research. — 1983. — Vol. 88. — P. 365–380.

[25] Lyster P.M., Leboeuf J.N. A fluid-ion and particle-electron model for low-frequency plasma instabilities // J. Computational Physics. — 1992. — Vol. 102. — P. 180–193.

[26] McIlwain C.E. Direct measurement of particles producing visible aurora // J. Geophysical Research. — 1960. — Vol. 65. — P. 2727–2747.

[27] Mozer F.S., Carlson C.W., Hudson M.K., et al. Observations of paired electrostatic shocks in the polar magnetosphere // Physical Review Letters. — 1977. — Vol. 38. — P. 292–295.

[28] Mozer F.S., Kletzing C.A. Direct observation of large, quasi-static, parallel electric fields in the auroral acceleration region // Geophysical Research Letters. — 1998. — Vol. 25, No. 10. — P. 1629–1632.

[29] Okuda H. Particle simulation models for low frequency microinstabilities in a magnetic field // Space Science Reviews. — 1985. — Vol. 42. — P. 41–52.

[30] Rankin R., Samson J.C., Tikhonchuk V.T. Parallel electric fields in dispersive shear Alfven waves in the dipolar magnetosphere // Geophysical Research Letters. — 1999. — Vol. 26. — P. 3601–3604.

[31] Rankin R., Samson J.C., Tikhonchuk V.T., Voronkov I. Auroral density fluctuations on dispersive field line resonances // J. Geophysical Research. — 1999. — Vol. 104, No. A3. — P. 4399–4410.

[32] Seyler C.E. A mathematical model of the structure and evolution of small-scale discrete auroral arcs // J. Geophysical Research. — 1990. — Vol. 95. — P. 17199–17215.

[33] Stern D.P. One-dimensional models of quasi-neutral parallel electric fields // J. Geophysical Research. — 1981. — Vol. 86, No. A7. — P. 5839–5860.

[34] Swift D.W. On the formation of auroral arcs and acceleration of auroral electrons // J. Geophysical Research. — 1975. — Vol. 80, No. 16. — P. 2096–2108.

[35] Temerin M., McFadden J., Boehm M., Carlson C.W., Lotko W. Production of flickering aurora and field-aligned electron flux by electromagnetic ion cyclotron waves // J. Geophysical Research. — 1986. — Vol. 91. — P. 5769–5792.

[36] Tikhonchuk V.T., Rankin R. Electron kinetic effects in standing shear Alfven waves // Physics of Plasmas. — 2000. — Vol. 7, No. 6. — P. 2630–2645.

[37] Vshivkova L.V. Numerical simulation of the multicomponent plasma dynamics // Vestnik of Novosibirsk State University. — 2003. — Vol. 3, No. 2. — P. 3–19.

[38] Winske D., Quest K.B. Electromagnetic ion beam instabilities: comparison of one- and two-dimensional simulations // J. Geophysical Research. — Vol. 91. — P. 8789–8797.

[39] Winske D., Yin L., Omidi N., Karimabadi H., Quest K.B. Hybrid simulation codes: past, present and future — a tutorial / J. Buchner, C.T. Dum, M. Scholer, eds. // Space Plasma Simulation. — Springer, 2003. — P. 136–165. — (Lecture Notes in Physics; 615).